NANO MICRO small

Supporting Information

for *Small*, DOI: 10.1002/smll.201702724

One-Way Particle Transport Using Oscillatory Flow in Asymmetric Traps

*Jaesung Lee and Mark A. Burns**

Supporting Information

Title One-Way Particle Transport using Oscillatory Flow in Asymmetric Traps

*Jaesung Lee and Mark A. Burns**

Table S1. The ratio of the unit flow (Q_{unit}) to total flow (Q_g) for various normalized trapping gap size. The row shift fraction (ε) of the trap array is 1/3.

Normalized trapping gap ($s^* = s/h$)	Q_{unit} / Q_g	$\eta = (Q_{unit}/Q_g)/\varepsilon$
0.1	0.2488	0.7464
0.2	0.3226	0.9678
0.3	0.3233	0.9699
0.4	0.3306	0.9918
0.5	0.3333	0.9999

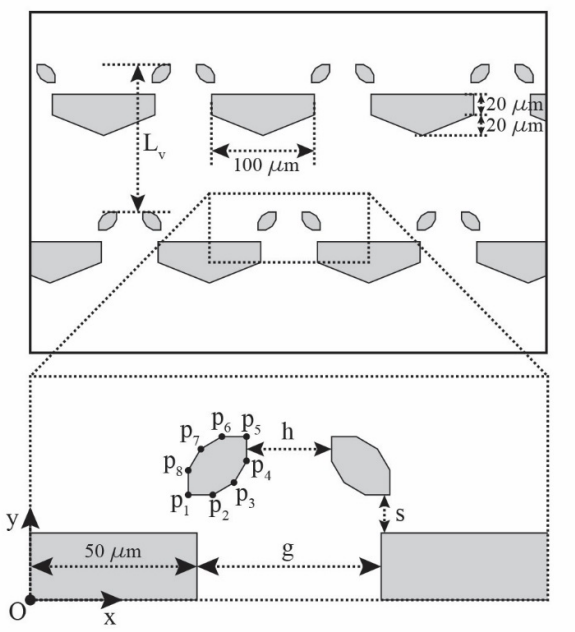

Figure S1. The dimension of the asymmetric trap array.

Table S2. Length and coordinates of the variables of Figure S1.

Variables	Coordinate [x , y]
L_v [μm]	2*[Round up (s + p_1(y) – p_5(y) + 40) by 5]
p_1	[50-(g-h)/2*tan(15^o) , s]
p_2	[54-(g-h)/2*tan(15^o) , s]
p_3	[50+(g-h)/2*(1-tan(15^o)) , s+(g-h)/2*tan(15^o)]
p_4	[50+(g-h)/2 , s+(g-h)/2*(1+tan(15^o))-4]
p_5	[50+(g-h)/2 , s+(g-h)/2*(1+tan(15^o))]
p_6	[46+(g-h)/2 , s+(g-h)/2*(1+tan(15^o))]
p_7	[50 , s+(g-h)/2]
p_8	[50-(g-h)/2*tan(15^o) , s+4]

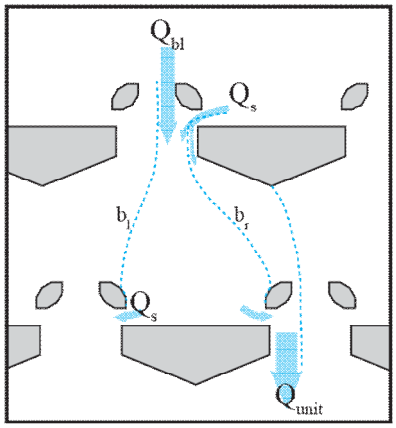

$$Q_{bl}+Q_s=Q_{unit}+Q_s \Rightarrow Q_{bl}=Q_{unit}$$

Figure S2. Modified mass balance relationship when $Q_s \leq Q_{unit} \leq 2Q_s$ at larger trapping gap size. Since the rightmost boundary streamline, b_r, of the capturing stream is outside the inter-trapping blocks gap (h), Q_{br} is equal to zero.

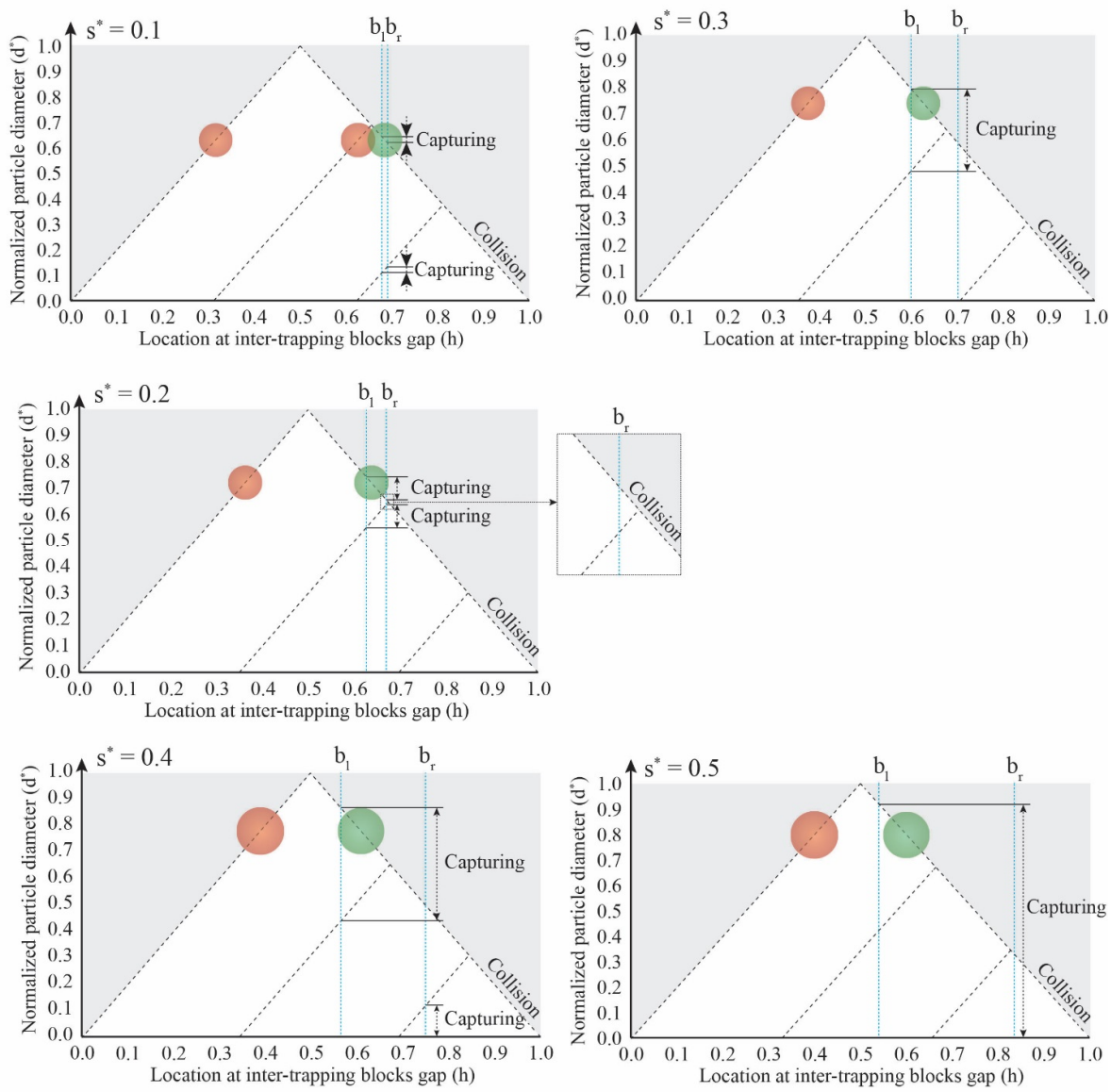

Figure S3. The lateral shift of the particle into the capturing stream at different trapping gap sizes ($0.1 \leq s^* \leq 0.5$)

Supplementary Note S1. Oscillation amplitude for the one-way particle transport

In principle, the oscillation amplitude, λ, needs to be greater than two vertical periods of asymmetric traps for one-way particle transport to occur. The amplitude of the fluid oscillation should be large enough to provide the possibility of capture during reverse flow (**Figure S4**a). Although the minimum amplitude for one-way particle transport varies with particle diameter, a convenient way to determine the amplitude is to have the amplitude greater than two vertical periods, i.e., the distance of 2/ε rows, of asymmetric traps (Figure S4b). Since the particles are captured while passing across a single period (1/ε rows of traps), and taking into account that no collisions occur in the region where the array changes the direction of the row shift, any amplitude greater than 2/ε rows can assure positive net displacement during one fluid oscillation. It is worthwhile to note that the alternating sign of the array shift angle at every vertical period of the traps was made in consideration of actual experiments (Supplementary NoteS3 and Figure S10).

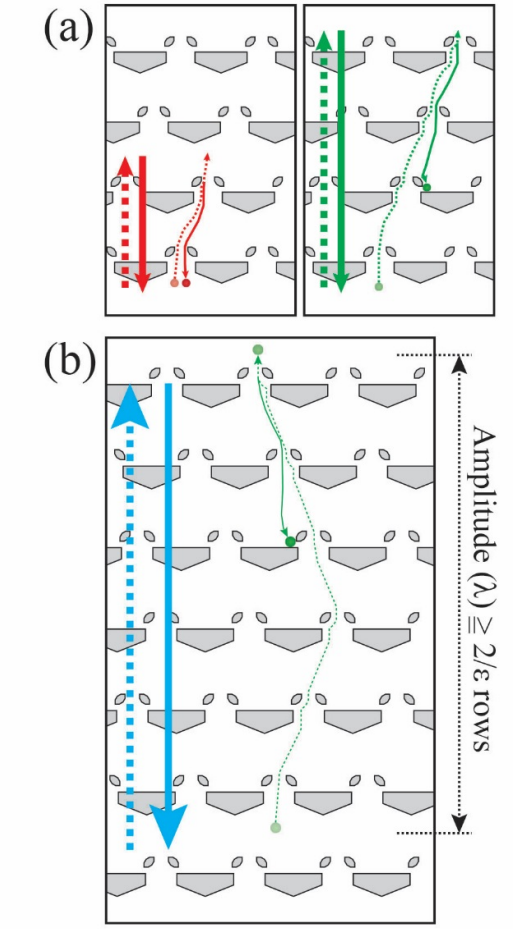

Figure S4. The amplitude (λ) of fluid oscillation should be greater than two vertical periods, the distance of 2/ε rows, of asymmetric traps. (a) Too small amplitude (red arrows) does not provide a chance of capture during reverse flow. On the other hand, long amplitudes (green arrows) can make positive net displacement. (b) Any amplitude greater than the distance of 2/ε rows can provide positive net displacement.

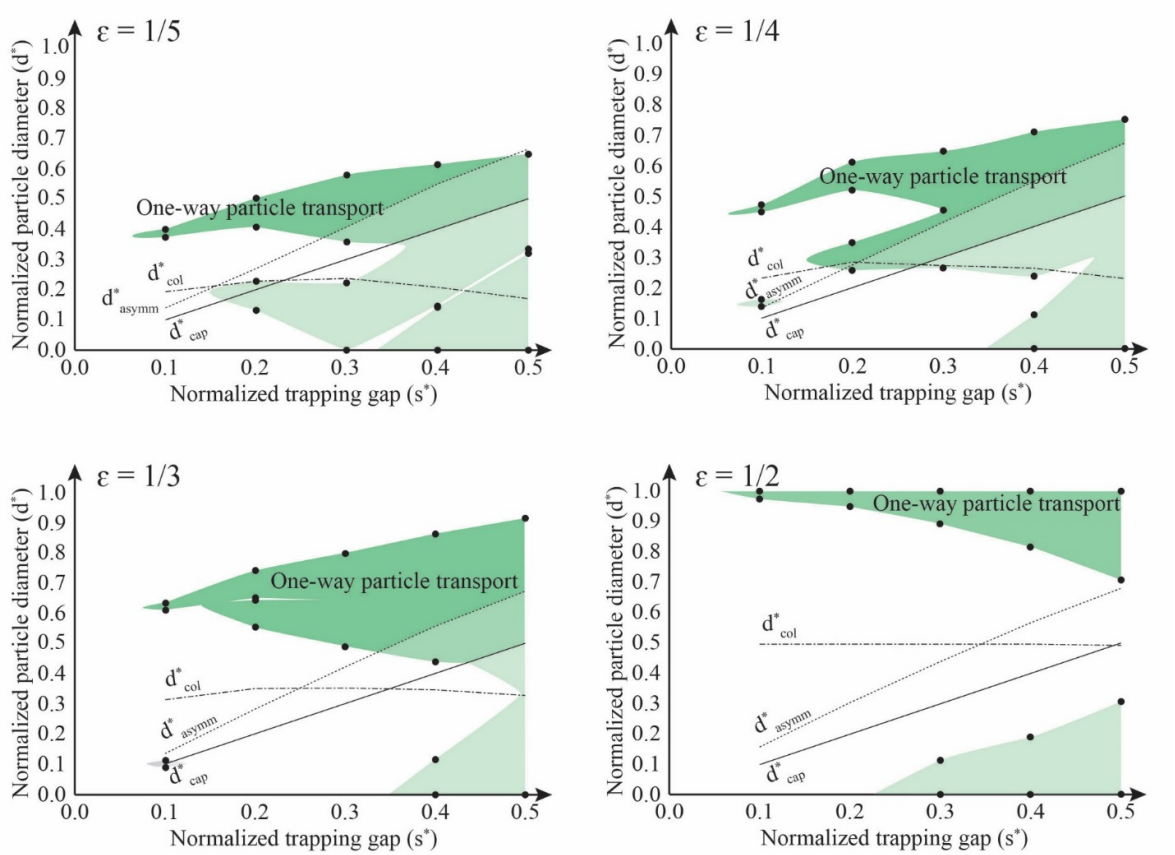

Figure S5. Phase diagrams at different row shift fractions (ε = 1/5, 1/4, 1/3, and 1/2). The black dots in the graphs are the intersections between the boundary streamlines of the capturing stream and the lateral locations of the particle center in reverse flow at five normalized trapping gap sizes (s* = 0.1, 0.2, 0.3, 0.4, and 0.5). The green area between the black dots becomes the diameter range for the lateral shift into the capturing stream in the reverse flow. It should be noted that the line between the calculated points was interpolated based on the trend of the diameter range at two trapping gap sizes (Supplementary Note S2).

Supplementary Note S2. The interpolation process for the trap-particle interaction phase diagram

First, we calculated the diameter range for the lateral shift into the capturing stream in reverse flow at various normalized trapping gaps ($s^* = 0.1$, 0.2, 0.3, 0.4, and 0.5 at $\varepsilon = 1/3$) (Figure S6a). Next, we connected the calculated points of two neighboring trapping gaps, and we adjusted and smoothed the line shape based on our conjecture (Figure S6b). In Figure S6b, we circled the region of the conjecture. The conjecture reflects two phenomena: 1) the diameter range of the capturing (or the non-capturing) region gradually disappears if the diameter range of the capturing region (or the non-capturing region) is not present at the neighboring trapping gap, and 2) sudden changes of the slope of the line present the change of the intersection point to calculate the diameter range. The regions I, II, IV, V, and VII are the examples of the first phenomenon, and the other regions, III and VI, were depicted based on the latter one. In more detail, in region I, as the trapping gap decreases from 0.1 to 0.0, the diameter range at the trapping gap of 0.1 must shrink and disappear because smaller trapping gap will reduce the width of the capturing stream (i.e. the distance between b_l and b_r in Figure S6c). Likewise, in the region II, the diameter range should disappear as the trapping gap decreases from 0.1 to 0.0. However, the diameter range in the region II should also be gradually reduced, and this region vanishes as the trapping gap increases to 0.2 because the capturing of the particle at the 3rd row disappears at the trapping gap of 0.2 (Figure S6c). This disappearance of the capturing can be attributed to the lateral shift of the capturing stream due to the increase in the vertical spacing of the traps. And, region IV came from the the non-capturing diameter range between two capturing diameter range at the trapping gap of 0.2. That non-capturing diameter range does not exist at the trapping gap of 0.1 and 0.3, so that region IV becomes sharply pointed to both directions of the trapping gap of 0.2.

The two islands, the capturing region (II) and the non-capturing region (IV), are non-significant in the practical use of the one-way particle transport. The capturing region (II) is below d^*_{asymm}, which means the particles in the region are supposed to have symmetric passage or symmetric capturing interaction that cannot show one-way particle transport (Figure S6d). For the non-capturing region (IV), the diameter range of the region is from 0.646 to 0.654, which is about 0.01 in d^*. Considering its small size, the non-capturing region (IV) would hardly prevent the particles from capturing unless the particles are very small compared to the inter-trapping blocks gap (i.e. particle diameter <1% of the inter-trapping blocks gap).

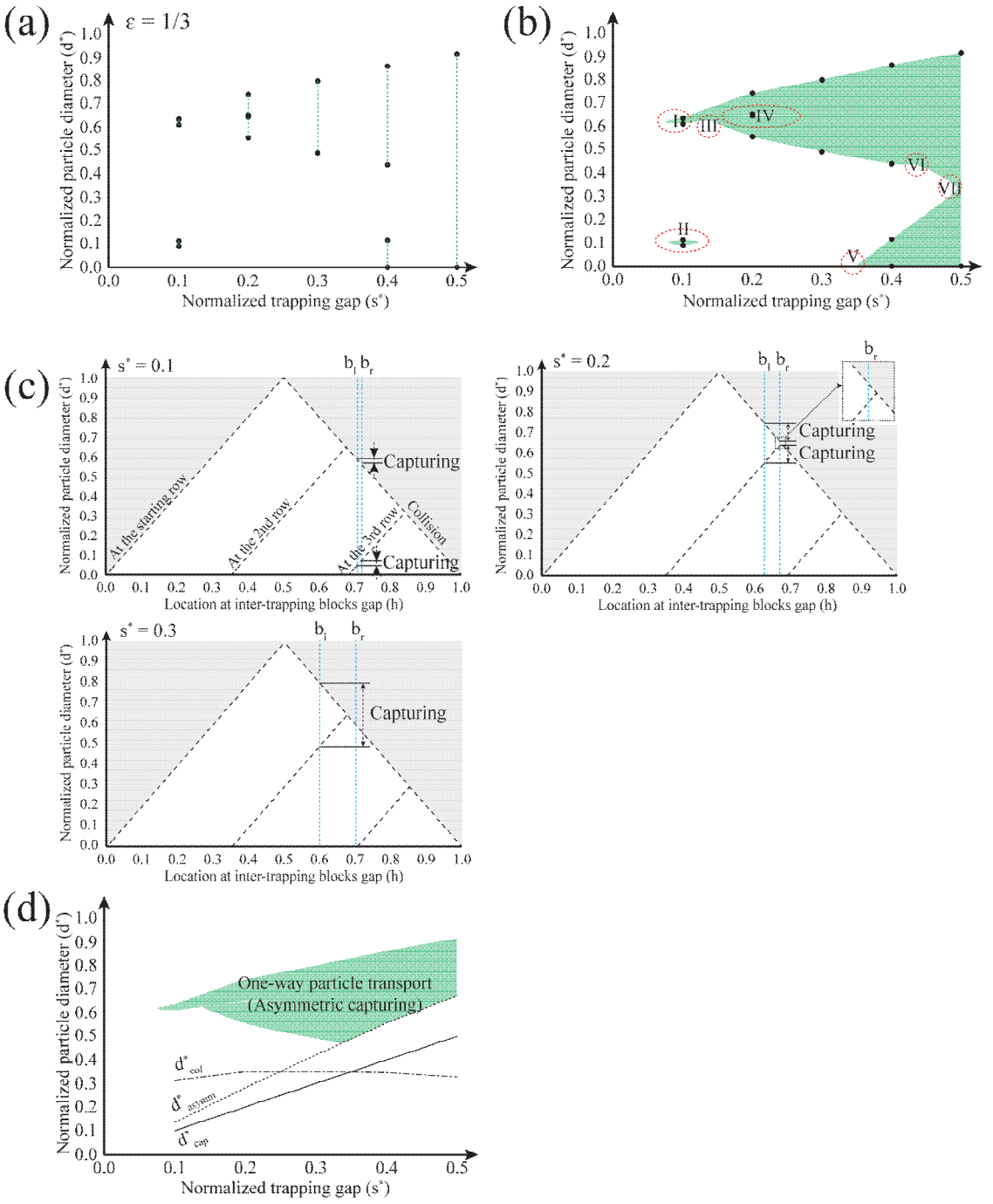

Figure S6. The interpolation for the trap-particle interaction phase diagram. (a) A raw graph of the diameter range (shown as green dashed lines) of the particles laterally shifted into the capturing stream at different trapping gaps (s^* = 0.1, 0.2, 0.3, 0.4, and 0.5). The diameter range was calculated from Figure S3. (b) The graph of the diameter range after the interpolation and smoothening. The calculated points of the neighboring trapping gaps were connected at first, and the slope of the connected line was further adjusted and smoothed based on our conjecture. The circled regions from I to VII present the conjected regions. The region I, II, IV, V, and VII were interpolated such that the diameter range of the capturing (or the non-capturing region) gradually disappears if the diameter range of the capturing region (or the non-capturing region) is not present at the next trapping gap. And, the sudden changes

of the slope of the lines in the region III and VI reflected the change of the intersection point at the edge of the diameter range. (c) The simplified version of Figure S3 to explain the region I, II and IV in more detail. (d) The region for the one-way particle transport after the critical diameters for the four conditions are applied. The capturing region (II) disappeared because it is below d^*_{asymm}. The diameter range of the non-capturing island in the region IV is from 0.646 to 0.654, which is about 0.01 in d^*. Considering its small size, the non-capturing region (IV) would hardly prevent the particles from capturing unless the particles are very small compared to the inter-trapping blocks gap (i.e. particle diameter <1% of the inter-trapping blocks gap).

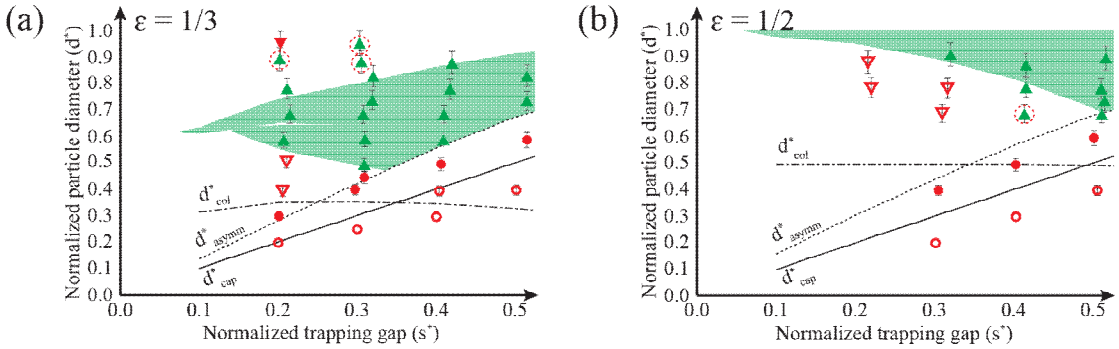

Figure S7. Experimental validation of the theoretical results. Theoretical prediction and experimentally validated trap-particle interaction dynamics in the arrays of row shift fraction (ε) of 1/3. The regions shaded in green are supposed to show one-way particle transport according to the theoretical results. Symbols: green triangles (▲) = one-way particle transport, inverted closed red triangles (▼) = trap skipping by bump mode, inverted open triangles (▽) = trap skipping by zig-zag mode , closed circles (●) = symmetric capturing, and open circles (○) = symmetric passage.

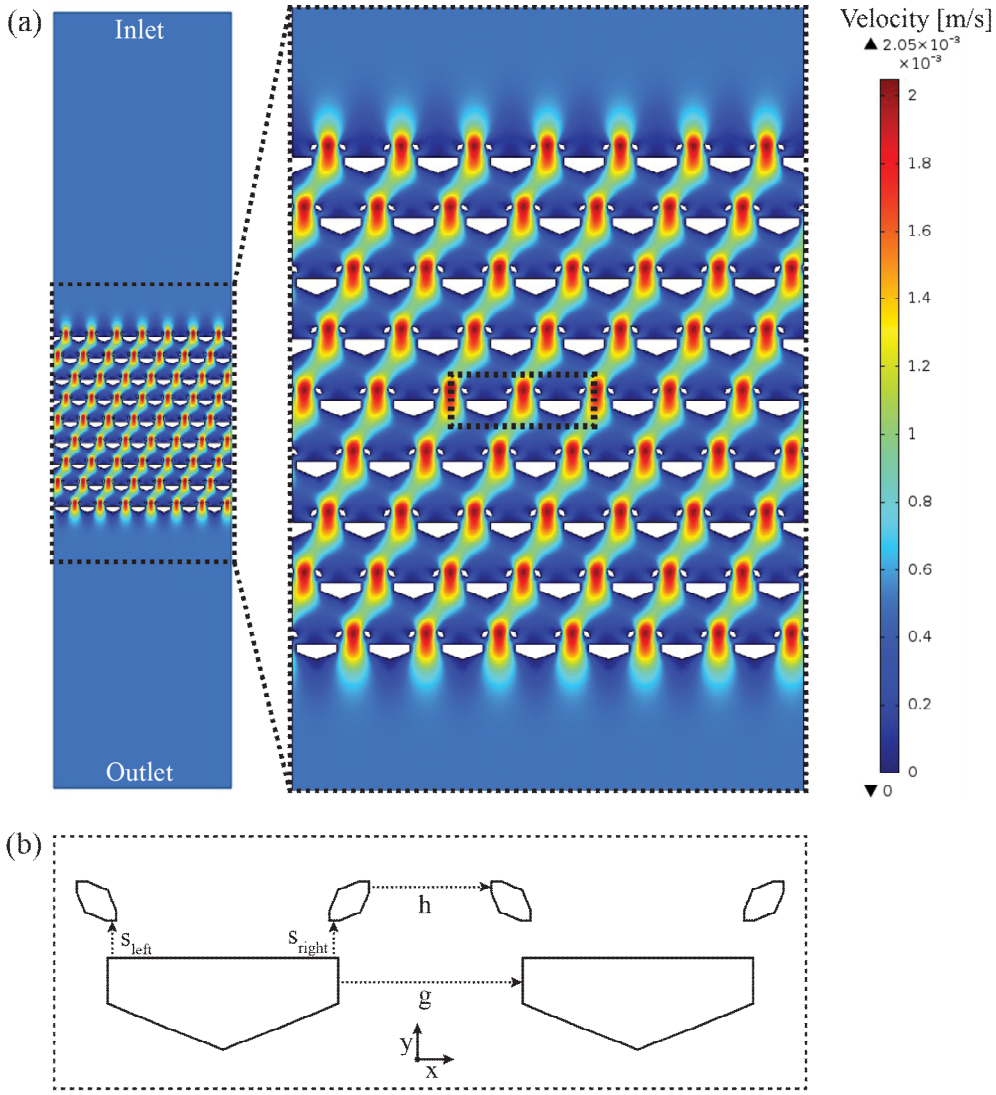

Figure S8. (a) Velocity plot of the Finite Element Method simulation results. Flat inlet and outlet profiles ensure average vertical velocity across the asymmetric trap array. The flow rate of each gap was calculated by averaging the flow rates obtained at five different locations in the central region of the array. The array dimension shown here is $\varepsilon = 1/3$, $g^* = 1.5$, and $s^* = 0.3$. (b) The regions of the velocity profile integration. Each two-dimensional volumetric flow rate was obtained via the mathematical integration of each flow profile along the dashed line shown above at each gap. For example, Q_s, the volumetric flow rate through the trapping gap, s (here, either s_{right} or s_{left}), was calculated by integrating the x-component of the velocity profile along s_{right}. This integration introduces some error because it ignores the contribution of the y-component of the flow profile to the flow rate. However, the difference between $2Q_s + Q_h$ and Q_g was found to be very small (<1% of Q_g), which assures the error can be ignored. The difference between the flow rates at s_{left} and s_{right} was also found to be small (~3% of Q_s). We also checked the effect of the no-slip condition on the balance between Q_ss at s_{left} and s_{right}, which we found that the difference between the two is insignificant (1% of Q_s). This small difference can be attributed to the large fluidic resistance of the trapping gap, s, compared to the resistance of the inter-trapping blocks gap, h. Since most of the fluid passes through h, the boundary conditions applied to the channel sidewall cause no significant difference between two Q_ss of the asymmetric trap.

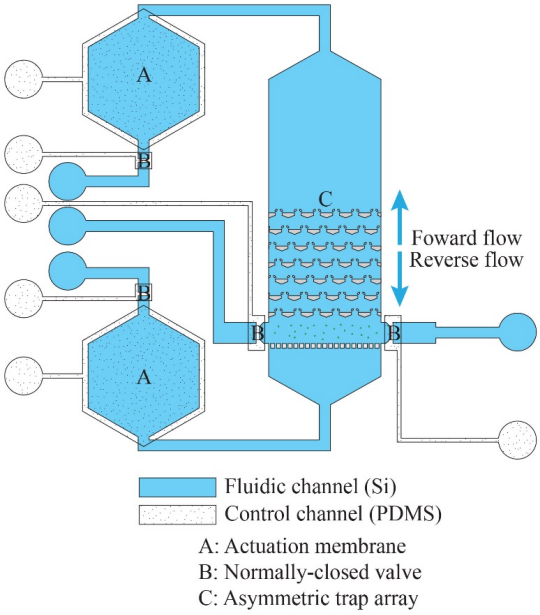

Figure S9. Device diagram. The device consists of three layers including a bottom fluidic channel, a top control channel, and a thin PDMS membrane separating the two channels.

Supplementary Note S3. Alternating the sign of row shift angle

Taking into account the experimental implementation of one-way particle transport, the sign of the row shift angle should be alternated to prevent undesired particle concentration at the region near the channel sidewall **(Figure S10)**. Large particles show bump mode transport, a type of particle transport following the direction of the row shift by capitalizing on the particle collision at every row of the trap array. Bump mode transport causes the area near the sidewall of the array that has only a single sign of the row shift angle to become crowded with particles. This unwanted particle concentration increases the probability of channel clogging and may cause errors in the operation of one-way particle transport. Alternating the sign of the row shift angle can minimize the particle crowding by guiding the particles to the opposite direction before they reach the sidewall area.

To keep the conditions for one-way particle transport unchanged, the sign of the row shift angle has to remain constant for at least $1/\varepsilon$ rows of the array. Although this design doubles the flow periodicity of the array from $1/\varepsilon$ rows to $2/\varepsilon$ rows, the conditions about the physical collision and the lateral shift into the capturing stream are viable in $1/\varepsilon$ rows so that the amplitude of $2/\varepsilon$ rows achieves one-way particle transport. By placing one row of traps at the inlet of the array and adding $1/\varepsilon$ rows of the traps with alternating signs of the row shift angle, an array with the sign of the row shift angle fixed for $1/\varepsilon$ trap rows can be designed.

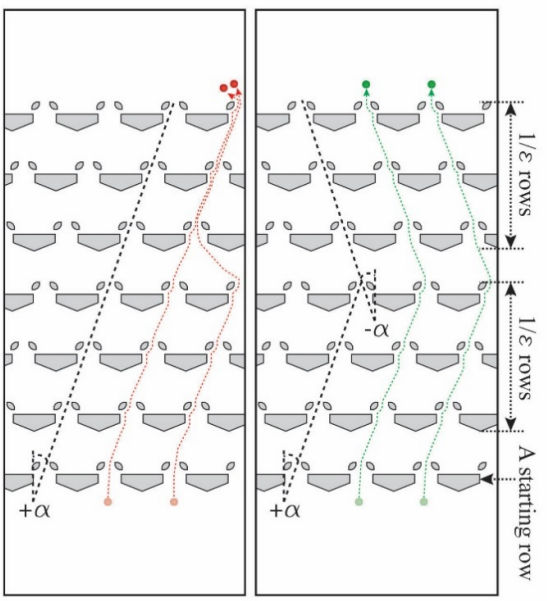

Figure S10. Undesired local particle concentration (left) in the area near the right channel sidewall can be avoided by alternating the sign of the row shift angle from +α to –α, or vice versa (right). The array was designed to have a fixed sign of the row shift angle for a single vertical period (1/ε rows) of the traps. This design allows the results of the d^*_{col} and the lateral shift into the capturing stream to remain valid while alternating the sign of the row shift angle.

Movie S1. One-Way Particle Transport

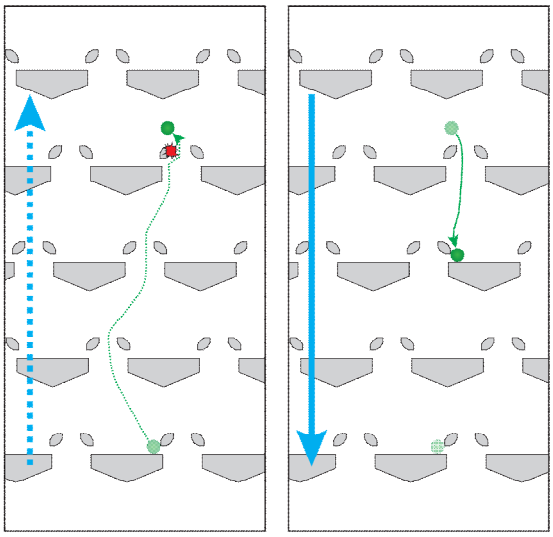

Figure S11. Schematic diagram of one-way particle transport

Movie S2. Symmetric Capturing

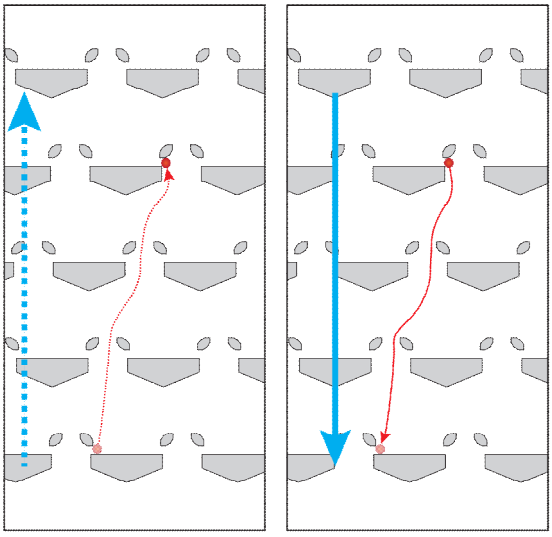

Figure S12. Schematic diagram of symmetric capturing

Movie S3. Symmetric Passage

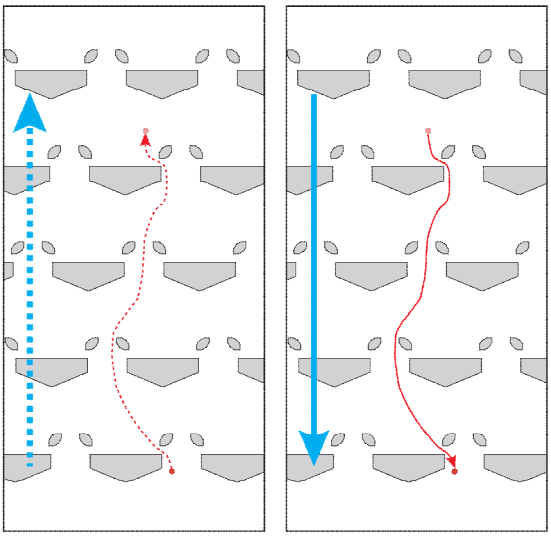

Figure S13. Schematic diagram of symmetric passage

Movie S4. Trap Skipping (Zig-zag mode transport)

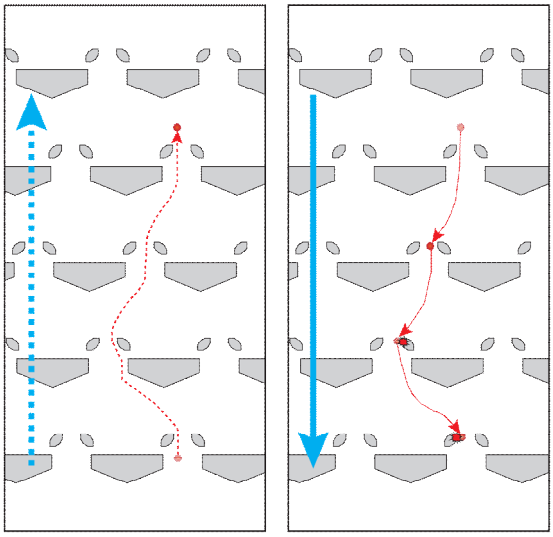

Figure S14. Schematic diagram of trap skipping in zig-zag mode

Movie S5. Trap Skipping (Bump mode transport)

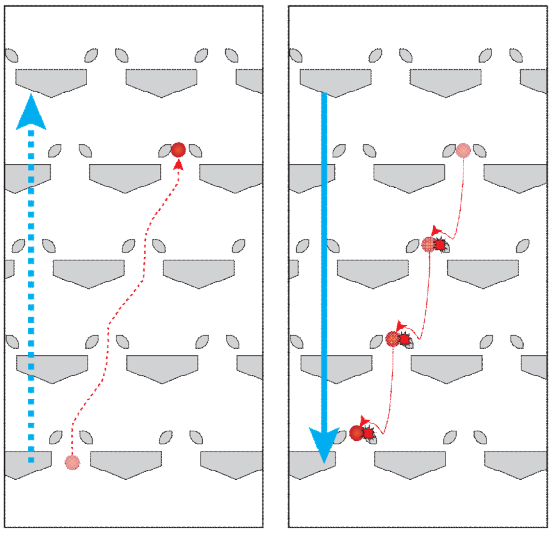

Figure S15. Schematic diagram of trap skipping in bump mode

Movie S6. Clogging and Releasing

*All of the movies are ten times slower than real time.